OPTOELECTRONICS AND ADVANCED MATERIALS – RAPID COMMUNICATIONS Vol. 15, No. 11-12, November-December 2021, p. 555-563

A compact twofold spoon-shaped antenna for ultra-wideband (UWB) applications

ISMAIL HOSSAIN[a,*], MD SAMSUZZAMAN[b,*], NORBAHIAH MISRAN[c], GOLAM MD. MURADUL BASHIR[b], CHINMAY BEPERY[b], MOHAMMAD TARIQUL ISLAM[c,*]

[a]*Space Science Center (ANGKASA), Universiti Kebangsaan Malaysia, 43600 UKM Bangi, Selangor, Malaysia*

[b]*Faculty of Computer Science and Engineering, Patuakhali Science and Technology University, Bangladesh*

[c]*Dept. of Electrical, Electronic and Systems Engineering, Faculty of Engineering and Built Environment, Universiti Kebangsaan Malaysia, Malaysia*

This article presents a twofold spoon-shaped UWB antenna compact with a spoon-shaped radiator patch and an inverted cone-shaped ground plane. The proposed antenna achieved 4 dBi gain, 80% efficiency, and 7.6 GHz bandwidth in between 2.80–11GHz operating frequency band for the reflection coefficient of S_{11}<-10 dB. FR-4 substrate is used to design and fabricate the proposed prototype with compact dimensions of 20 × 20 × 1.6 mm^3, where relative permittivity and loss tangent value is 4.30 and 0.02, respectively. Gain and radiation characteristics are measured using the 3D electromagnetic simulator CST microwave studio 2018 that's offers E-field and H-field omnidirectional patterns. The proposed antenna's impedance bandwidth, radiation patterns, peak gain, and time-domain performance is analyzed to evaluate its appropriateness in UWB communication. Finally, the measured results are agreed with the simulated results.

(Received June 18, 2021; accepted November 24, 2021)

Keywords: Bluetooth, Twofold spoon-shaped, Ultra-wideband, Integrated antenna, Gain measurement, Wireless communication

1. Introduction

Ultra-wideband (UWB) antenna became more popular to researchers since the frequency band of 3.1 to 10.6 GHz was declared unlicensed-band by the federal communication commission in 2002. In addition, the UWB antenna is used widely both in academics and enterprises for its high-speed data transmission rate, low spectral power density, and less interference [1]. Thus, ultra-wideband radio communication technology is conducted to high-speed (more than 100 Mbps) communication. Still, a predominant mission is to design a compact UWB antenna with immoderate bandwidth and high efficiency and gain [2]. Therefore, researchers introduced different shapes of UWB antennas to overcome those limitations, such as rectangle [3], ellipse [4], octagonal [5], planner UWB [6], binomial curve [7], rhombus [8], and bow tie antenna [9].

A spiral-shaped UWB is designed, and then it is investigated theoretically and experimentally in the frequency of 1.7-6.0 GHz [10]. Finally, a bow-tie antenna is designed to make it reasonable for UWB applications like Wi-Fi, WLAN, WiMAX, television, radiosonde, navigational aids, radar, and satellite communication. As a result, numerous performance factors are improved, like return loss (S_{11}), voltage standing wave ratio (VSWR), and bandwidth compared to conventional bow-tie antennas without slots [11]. Numerous UWB antenna designs have been studies such as triangle [12], circle [13], fractal [14], sensor-based UWB [15], slotted UWB antenna [16], UWB monopole antenna [17], directional UWB antenna [18], parasitic resonator-based antenna [19]. An antenna's configurable notch band selectivity can be a proper technique, but this technique increases the antenna size. A fractal antenna has self-similarity, and space-filling characteristics play an essential function in designing low-profile broadband and multiband antennas. Therefore, the designers intended numerous fractal geometries, such as Sierpinski fractals, Minkowski fractals, Hilbert curves, and Koch recursive tree structures. A Minkowski-like fractal is a fractal geometry wideband antenna using more than one resonance phenomenon [20]. In addition, designers apply several techniques to improve the UWB antenna performance, for example, inserting a stub on one side of a circular patch, calculating partial metal fields [21], adding slots on one side of the radiation element [22].

Vivaldi antennas have two variants, coplanar and antipodal structures [23], and this antenna is widely used for planar configuration, impedance bandwidth, and low profile [24]. A tapered slot antenna is considered a suitable UWB antenna because of its sentential amount of operational bandwidth, high gin, radiation directivity, and planar configuration. The specific variations of tapered slot antenna (TSA) profile and substantially tapered shape, antipodal is designed with different feeding methods to excite TSA slots and have been investigated in detail [25],[26],[27], respectively. A two-fold spoon-shaped UWB antenna is presented in this article for short-distance wireless communication. The radiating and ground layers are fascinated on both sides of FR-4 dielectric material, where a 50 Ω microstrip feed line is used.

Furthermore, we study the development of FR-4 substrate-based antenna for ultra-wideband applications, focusing on various significant antenna parameters such as reflection coefficients (S_{11}), radiation patterns, VSWR, antenna gain, and directivity. Compared to the whole ground plane with an inverted cone-shaped ground plane is achieved more wide operating bandwidth. Therefore, the designed antenna has a wide bandwidth (2.80 GHz to 11GHz) due to appropriate impedance matching between the ground plane and patch. Computer Simulation Technology CST Microwave Studio Suite 2018 is used to designed and investigate the proposed UWB antenna.

2. Design layout of the single antenna structure

A compact twofold spoon-shaped UWB antenna has been designed and simplified characteristics in this article. The ultimate intention of developing an antenna is to increase bandwidth, gain, efficiency, and directive radiation pattern. Fig. 1(a, b) shows the proposed antenna's geometrical shape. The antenna is designed and simulated using the Advanced Design System (ADS). The proposed antenna has been used as the lowest cost epoxy FR-4 dielectric substrate, and the relative permittivity ε_r is 4.3, the loss tangent δ = 0.02, and the thickness h = 1.6 mm. The radiator looks twofold spoon-shaped, and the ground plane is inverted cone-shaped. Adjust the radius of the twofold spoon-shaped radiating patch to the near center of the inverted cone-shape ground plane, and the position of the patch will vary until the characteristic impedance bandwidth of VSWR< 2 is obtained in the lower frequency band. Df denotes the appropriate distance between the feed line and the left edge of the structure.

In addition, the antenna width and effective dielectric constant ε_{eff} of the material affect the lower operating frequency band. However, the proposed twofold spoon-shaped resonator-based antenna achieves the ultra-wideband (UWB) characteristics. By using [28] this formula, the antenna width and length are calculated. The whole dimension of the proposed compact UWB antenna is 20 × 20 × 1.6 mm^3. The twofold spoon-shaped patch and the inverted cone-shaped ground plane are designed on the substrate's topside and the backside, where a twofold spoon-shaped patch is working as a main radiating element of the proposed UWB antenna. In addition, an inverted cone-shaped ground plane is placed in the lower half position of the backside of the substrate layer used to increase the antenna radiation directivity. The ground plane width (W) is 20 mm, and the distance between the circular slots and the bottom of the ground plane (G) is 0.035 mm. Thus, W_F denotes the width of the feed line, and its value is 1.00 mm, and it's directly connected to the radiating patch and fed with a 50 Ω SMA connector. The dielectric constant and electrical conductivity of the SMA connector is 2.08 and 4.62 × 104 S/m, respectively. The antenna parameter Q_4, which indicates the gap between the patch and bottom edge of the ground plane, substantially improves the overall bandwidth. The Q_4 parameter value is 5.00 mm. The antenna parameter Q4 is used to indicate the gap between the lower edge of the patch and the bottom edge of the ground plane. The Q4 parameter has a significance to improve the overall bandwidth, and its value is 5.00 mm. The proposed compact antenna has a 0.2 ns group delay across UWB frequencies. By using [28] this formula, the antenna width and length are calculated.

$$W = \frac{c}{2 f_0 \sqrt{\frac{\varepsilon_r + 1}{2}}} \tag{1}$$

$$\varepsilon_{eff} = \frac{\varepsilon_r + 1}{2} + \frac{\varepsilon_r - 1}{2}\left[\frac{1}{\sqrt{1 + 12\left(\frac{h}{w}\right)}}\right] \tag{2}$$

$$L = \frac{c}{2 f_0 \sqrt{\varepsilon_{eff}}} = -0.824h\left(\frac{\left(\varepsilon_{eff} + 0.3\right)\left(\frac{w}{h} + 0.264\right)}{\left(\varepsilon_{eff} - 0.258\right)\left(\frac{w}{h} + 0.8\right)}\right) \tag{3}$$

Here, *c* represents the speed of light and f_o represents the resonance frequencies.

2.1. Detail description of antenna parameters design

Some significant antenna parameters are listed in Table 1, and the geometric layout of the proposed antenna is shown in Fig. 1(a, b). The length and width of the proposed antenna are denoted by W and L, and its value is 20 mm, 20 mm, respectively. The distance between the bottom left corner and left edge of the feed is denoted by $D_{F,}$ and its value is D_F =11.5 mm. The microstrip feed line has a length of L_F=6.1095 mm, and an SMA connector is connected to the port of the microstrip feed line with 50 **Ω** characteristics impedance. G denotes the gap between the circular shape slot and the bottom of the ground plane, and the value of this parameter is 0.05 mm. Next, a twofold spoon-shaped patch is placed nearly close to the right edge of the proposed UWB antenna. R2 and R3 denote the outer and inner radius of twofold spoon-shaped resonators, and the value of these parameters is 3.1025 mm and 2.5014 mm, respectively. Subsequently, a half circular-shaped slot has been cut with an R1 (R1=9.9 mm) radius at the lower portion of the ground plane. Q1 represents the distance between the left-middle of the ground plane and the triangular-shaped slot, and its value is 5.49 mm. Then, another triangular-shaped slot has cut from the middle to top position on the ground plane where Q2 denotes the length of one arm of the triangular shape, and its value is 2.836 mm. The parameter Q3 represents the distance between the right middle of the ground plane and the radiating patch, and the value of the Q3 parameter is 7 mm. Q4 denotes the distance between the lower edge of the radiating patch and the bottom middle portion of the ground plane, and its value is 5.5 mm.

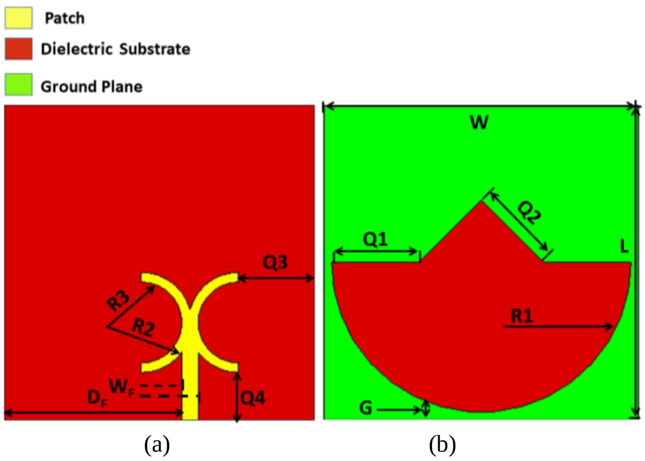

Fig. 1. Geometric layout of the proposed antenna: (a) Front view, (b) Back view (color online)

Table 1. The parameter list of the proposed UWB antenna

Parameters	value (mm)	Parameters	value (mm)
W	20	*Q1*	5.49
L	20	*Q2*	5.66
R1	9.98	*Q3*	7
R2	3.1025	*Q4*	5.5
R3	2.5014	*G*	0.5
L_F	6.2	H_S	1.6
W_F	1	*h*	0.035
D_F	11.50		

2.2. Parametric study of the proposed antenna

Some significant parameters need to modify due to enhancing the reflection coefficient under -10 dB, improving gain and antenna bandwidth. A twofold spoon-shaped radiating patch and ground plane are facing 180^o each other, and the final design of the proposed antenna is illustrated in Fig. 1. The width and length of the proposed antenna are denoted by W, and L respectively. A half-circular shape slot and a triangular-shaped slot are interlined in the ground plane. Thus, the radius of a half-circular shape slot and a triangular-shaped slot is denoted by R1 and Q2, respectively. R2 and R3, respectively, represent the outer radius and inner radius of the spoon-shaped patch. The distance between the circular-shaped slot and the bottom edge of the ground plane is denoted by G, and Q4 represents the distance between the twofold spoon-shaped patch and the bottom of the proposed antenna. Finally, Q3 represents the distance between the right edges to the upper point of the patch, and the left edge to feed line distance is defined by D_F. It observed that modifying any parameter value affects the reflection coefficient (S_{11}), gain, overall antenna performance, etc. Therefore, we have investigated the effect of Q1 and R2 parameters variation on the reflection coefficient of the proposed antenna shown in Fig. 2(a, b).

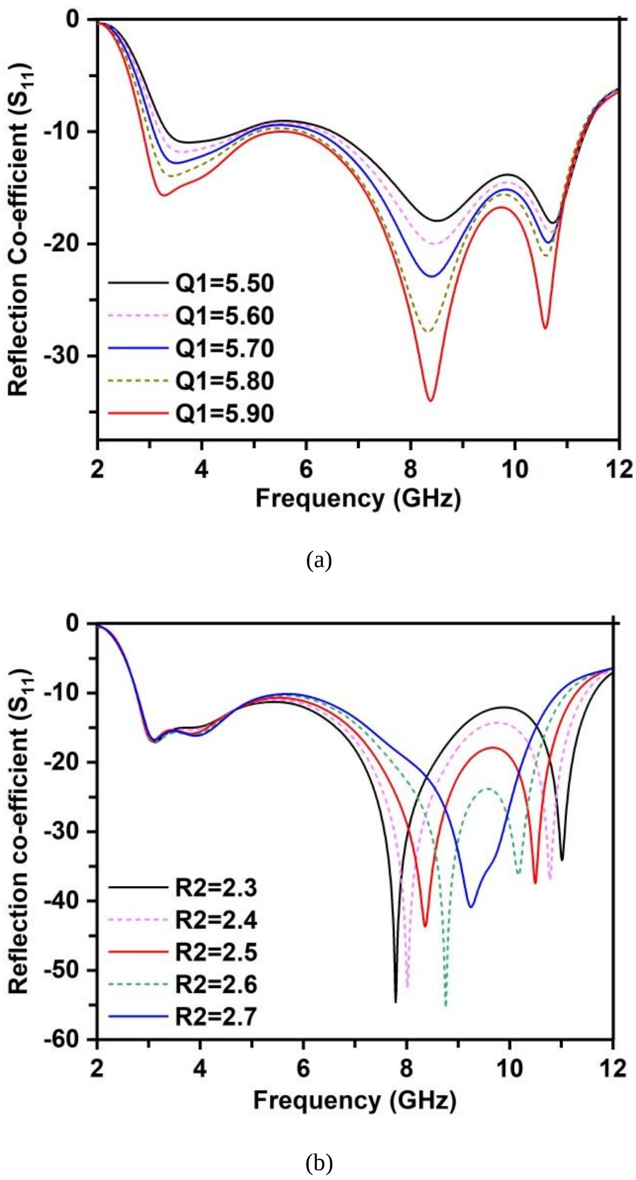

Fig. 2. (a) Radius of circular-cut of the ground plane R1, (b) Outer radius of the spoon-shaped patch R2 (color online)

3. Reflection coefficient effect

In this section, the scattering parameters of the design are analyzed, and the simulation result of a twofold spoon-shaped compact ultra-wideband antenna is presented. Generally, return loss refers to the reflection coefficient, which S_{11} denotes. The return loss (S_{11}) represents how much power is reflected from the proposed antenna and describes the input-output relationship between ports. The reflection coefficient (S_{11}) should be at least -10 dB to perform the proposed antenna efficiently; if the reflection coefficient (S_{11}) power is 0 dB, then all the power is reflected in the antenna. Thus, the lower value of the reflection coefficient (S_{11}) represents the better performance of the proposed antenna. Initially set Q1 parameter value 5.50 mm and observed the reflection co-efficiency curve. The lower frequency operates at 3.3-4.65 GHz, and the higher frequency operates at 6.51-11 GHz. Therefore, the reflection coefficient (S_{11}) goes down in the frequency range of 3.3-4.65 GHz and 6.51-11 GHz that does not cover the UWB frequency range, and at the resonance frequency of 3.74 GHz and 8.47GHz, we found its S_{11} value is -10.96 dB, and -17.96 dB shows in Fig. 2a. When we set the Q1 parameter value 5.60 mm, then the reflection coefficient (S_{11}) curve shows the lower frequency shifted from 3.3 GHz to 3.22 GHz, and the maximum -2.01 dB return loss is exhibited at 8.45 GHz frequency. After that, the Q1 parameter value is increased with a step size of 0.10 mm then the reflection coefficient (S_{11}) curve goes downward from -10 dB. If we change the Q1 parameter value to 5.70 mm, 5.80 mm, and 5.90 mm, then the proposed antenna shows the reflection coefficient (S_{11}) -23.03 dB, -27.822 dB, and -33.822 dB at the resonance frequency of 8.38 GHz, 8.30 GHz, and 8.35 GHz, respectively. We get the most acceptable value of the Q1 parameter at Q1= 5.90 mm and a large operating frequency band (2.86-11GHz), which covers the UWB frequency band from 3.00 to 10.6 GHz. The frequency versus return loss 2 D plot of the proposed UWB antenna is shown in Fig. 2(a,b). The outer radius R2 of the spoon-shaped patch is another critical parameter; if we increase the R2 value with a step size of 0.10 mm, then the reflection co-efficiency S_{11}curve right shift is observed. The right shift of the reflection coefficient (S_{11}) curve is observed by tuning the R2 parameter values 2.3, 2.4, 2.5, 2.6, and 2.7 mm with the increasing of R2 parameter, and the resonance frequency also increases by 7.79, 8.00, 8.37, and 8.72, 9.22 GHz, respectively. This modification also helps to enhance the radiation directivity and the reflection co-efficient curve, which is slightly far away from -10 dB. However, if we increase the R2 parameter value, then the current-conducting paths also increase. It is observed that the gain is gradually increased concerning frequencies from 2.80 GHz to 7.50 GHz, 8.80 GHz to 9.45 GHz, and 10.5 GHz to 11 GHz. Finally, the proposed UWB antenna achieves 5.8 dBi maximum gains. However, this circular cut of the ground plane (Q2) and outer radius of the spoon-shaped patch has a substantial effect on the surface current distribution that supports achieving the UWB (2.80-11GHz) frequency band.

3.1. E-field, H-field, and surface current analysis

The electric field, magnetic field, and surface current distributions are helpful to understand structural behavior. Fig. 3(a, b, c) illustrates the proposed structure's E- field, H- field, and surface current. Red colure indicates the high density of e-field, h-field, and surface current, whereby orange, yellow, green, and blue colure means lower high, medium, lower medium, and less intensity. At the frequency of 2.78 GHz, high intensity is noticed at the top portion of the twofold spoon-shaped radiating patch shown in Fig. 3(b). After that, at 4.63 GHz frequency, the field intensity is decreased, and only at the edge of a two-fold spoon-shaped radiator patch, the low field intensity observed, shown in Fig. 3(a). The high field intensity is indicated by red colure, which means that the point electric charge is well distributed. This phenomenon occurs because current flows throw the patches and the direction of recent flow changes concerning frequency. The same effect is observed in the h-field pattern presented in Fig. 3(b). A comparison of the e-field pattern is illustrated in Fig. 3(a), with the h-field pattern shown in Fig. 3(b). It is noticeable that where the h-field has minor variation, the electric field intensity is high. The electric field, magnetic field, and surface current distribution of the proposed UWB antenna are demonstrated in Fig. 3(a, b, c), corresponding to the significant resonance frequencies of 3 GHz and 5 GHz, respectively. This study is conducted on CST Microwave Studio 2019 simulator software to observe the electric field, magnetic field, and surface current distributions. The maximum prevailing current is noticed at the center of the twofold spoon-shaped patch element at 3 GHz frequency shown in Fig. 3c. But moderate current conduction region was observed at the left and right edge of the inverted cone-shaped ground plane and the radiating patch at 5 GHz frequency. But at 5 GHz frequency, the moderate current conduction region was observed at the left-center and right-center of the inverted cone-shaped ground plane and the center of the radiating patch. The proposed UWB antenna's current variation significantly affects the bandwidth, gain, efficiency, and radiation pattern. In addition, the incidence of a twofold spoon-shaped patch portion changes the current travel path and modifies the antenna functions essentially to extend the upper operating frequency range.

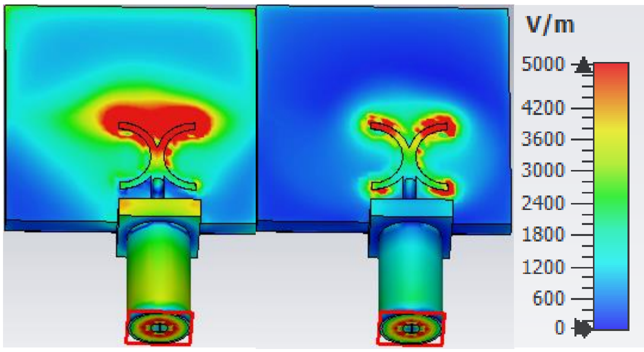

(a). E- field at 3 GHz, 5 GHz

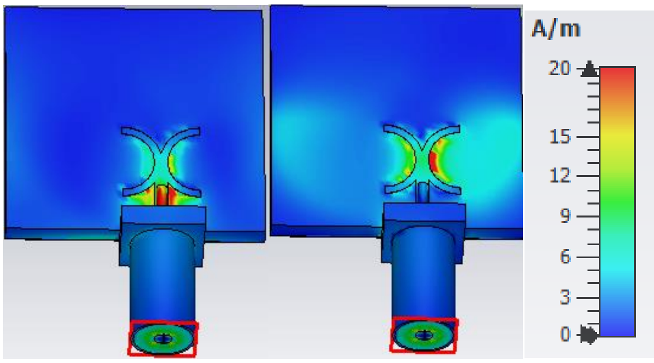

(b). H- field at 3 GHz, 5 GHz

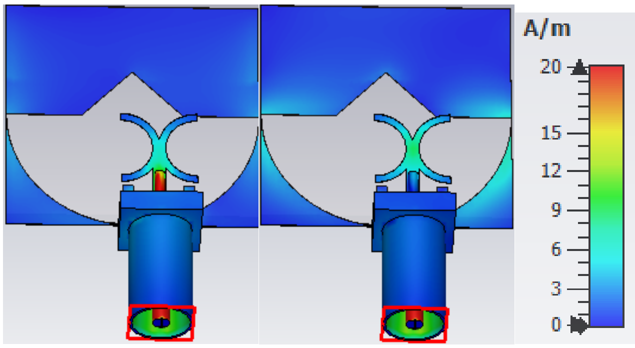

(c). at 3 GHz, at 5 GHz

Fig. 3. (a) E-field, (b) H-field, (c) Surface current distributions (color online)

3.2. Performance analysis of the antenna

The proposed work has been distinguished from other related ultra-wideband (UWB) antennas presented in Table 2. The proposed UWB antenna comprises a twofold spoon-shaped patch that works as a main radiating element to achieve a wide band. In addition, an inverted cone-shaped ground plane is designed on the backside of the proposed antenna. The proposed antenna covers the frequency band of C, X, Ku of the UWB microwave frequency spectrum. Thus, some antennas are reported high bandwidth, and they are substantially in dimensions compared to the proposed ones reported in Table 2 individually. In addition, the performance of the proposed antenna is increased, and miniature size, gain, bandwidth, and lower operating frequency are compared to those described in the previous literature. Therefore, the proposed twofold spoon-shaped can be suitable for WLAN / WiMAX / UWB wireless communication.

3.3. Gain and radiation efficiency v/s frequency

The frequency versus gain and radiation efficiency of the proposed spoon-shaped UWB is shown in Fig. 4(a, b). The proposed antenna achieved 4 dBi gains at 6 GHz frequency and up to 89% efficiency in the operating frequency. The following equation helps to understand the gain and radiation efficiency behavior of the proposed UWB antenna.

$$Gain = \eta D \tag{4}$$

where η is the efficiency and D is the directivity of the antenna.

$$D = \frac{4\pi A}{\lambda^2} \quad (5)$$

where A is the aperture area and λ is the wavelength. $\lambda = c/f$ where c is the speed of light and f is the frequency.

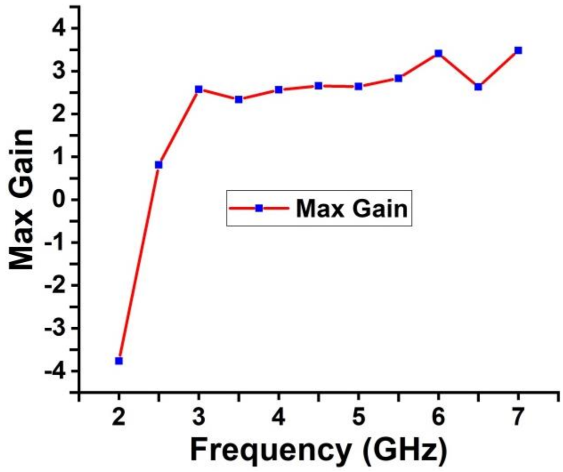

(a)

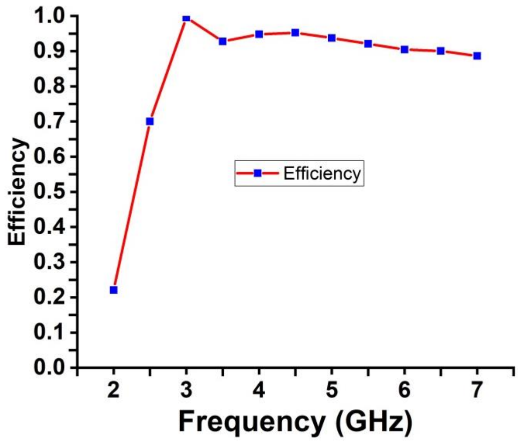

(b)

Fig. 4. (a) Gain v/s frequency curve (b) Efficiency v/s frequency (color online)

This study observed that the directivity (D) is proportional to the square of the frequency. Hence, D has increased the frequency, which is observed in the gain curve from figure (a). Since the electrical size of the antenna is large at higher frequencies, improving the directional properties of the antenna is observed. Therefore, initially, the radiation efficiency of the antenna increases with respect to the frequency, but as the frequency increases, the dielectric losses of the antenna increase that is inversely proportional to the efficiency of the radiation.

4. Results and discussion

The fabricated prototype of the proposed structure is shown in Fig. 5(a, b). The simulated and measured result of the reflection coefficient (S_{11}) of the proposed UWB antenna is presented in Fig. 6. The proposed UWB antenna shows a bandwidth of 7.6 GHz between 2.80-11GHz, and where the most significant points are at 2.78 GHz, 4.63 GHz, and 6.5 GHz, respectively. Subsequently, the prototype antenna's reflection coefficient (S_{11}) was measured by a vector network analyzer (N5227A). The measured prototype exhibited a 4.6 GHz bandwidth and found a resonance frequency at 3.0 GHz.

Moreover, three resonances were found from the measured data at the frequency of 3.7, 65, and 8.3 GHz, respectively. The return loss (S_{11}) curve shows that the impedance is matched over the entire frequency spectrum. The highest resonances' return loss (S_{11}) is enough in simulated and measured -36dB and -27 dB, respectively. A slight difference observed between the measured, and simulated results can be considered tolerance of measurement and solder errors from the SMA connector with the radiator. However, the designed antennas are covered in the S-band, C-band, and X-band of the UWB microwave frequencies spectrum. The proposed antenna can be considered a suitable candidate for other WLAN / WiMAX/UWB fields and other wireless communications.

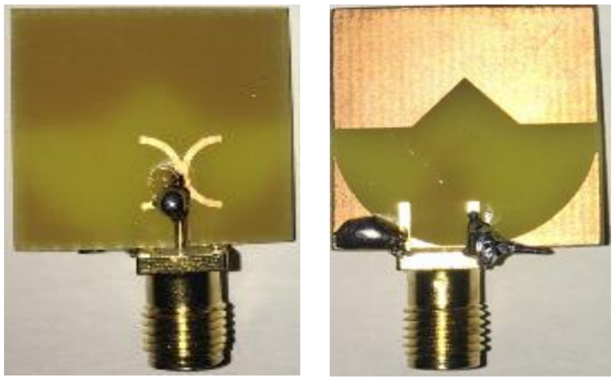

(a) (b)

Fig. 5. Front view and (b) Back view of the printed antenna (color online)

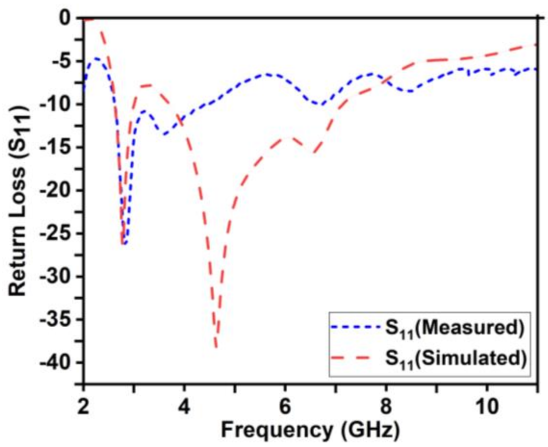

Fig. 6. Simulated and measured result of the reflection coefficient (S_{11}) or return loss (color online)

The radiation directivity of the proposed UWB antenna is improved due to the improvement of proper movement of surface current distribution with the help of half circular-shape slots on the ground plane and a twofold spoon-shaped radiating patch. When the twofold spoon-shaped patch's outer radius (R1) is increased, the reflection coefficient curve (S_{11}) goes down from -10dB for this result. The gain is also increased by creating a proper surface current movement path on the ground plane and radiating patch. The radiation pattern is a property of measuring the transmission/receiving characteristics and maximum energy in the direction of an antenna. A radiation pattern of the proposed antenna is presented at the resonance frequency of 3 GHz and 5 GHz, shown in Fig. 7(a, b). The radiation pattern of the designed antenna is plotted in the E- and H- plane, where a spherical coordinate system is used to plot the graphs and both theta (θ) and phi (φ) to 90 degrees. In addition, antenna radiation patterns are designed in electric (E-) and magnetic (H-) fields, where a spherical coordinate system is used to plot the graph at θ= 90 and φ=90 degrees.

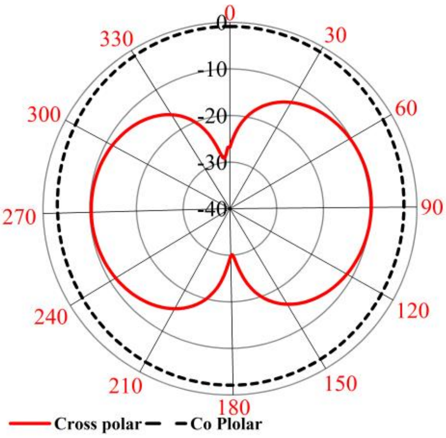

(a)

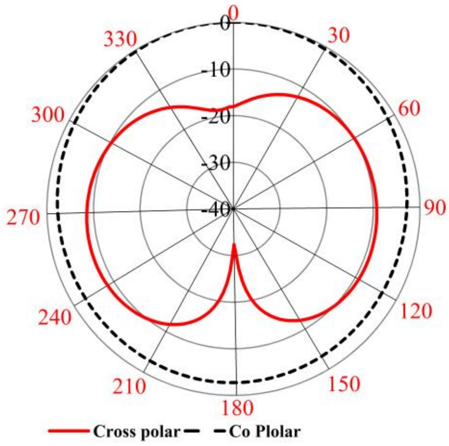

(b)

Fig. 7. The 2-dimensional radiation patterns of the proposed antenna at (a) 3 GHz; (b) 5 GHz (color online)

Table 2. Comparison over some previous work and present work

Ref. No	**Dimension(mm3)**	**Operating frequency (GHz)**	**Bandwidth (GHz)**	**Gain (dB)**	**Applications**
[6]	30 × 22 × 1.6 0.298λ × 0.187λ × 0.016λ	2.98–12.0	9.02	3.95	UWB
[7]	41.5 × 41.5 × 1.6 0.277λ × 0.277λ × 0.011λ	2.0–12.0	10	5.7	UWB
[8]	18 × 26 × 1.6 0.186λ × 0.269λ × 0.017λ	3.1–11.0	7.9	3	UWB
[26]	37 × 21 × 0.787 0.382λ × 0.217λ × 0.008λ	3.1–10.6	7.65	5.2	UWB
[27]	52 × 62.5 × 23.2 0.537λ × 0.646λ × 0.240λ	3.1–18.6	15.5	9.4	UWB
[29]	37 × 33 × 1.6 0.419λ × 0.374λ × 0.018λ	3.4–11	7.6	5.73	UWB
[30]	30 × 30 × 0.8 0.285λ × 0.285λ × 0.008λ	2.85–11.9	9.05	5	UWB
[31]	38.31 × 34.52 × 0.8 0.364λ × 0.328λ × 0.008λ	2.58–11.62	9.04	5	UWB
[32]	39 × 40 × 1.6 0.338λ × 0.347λ × 0.014λ	2.6-12.3	9.7	5.52	UWB
[33]	22 × 24 ×1.6 0.226λ × 0.246λ × 0.016λ	3.08- 11	5.5	4	UWB
[34]	27 × 23.5 × 1.6 0.297λ × 0.259λ × 0.018λ	3.3-20	16.7	5.11	UWB
[35]	14.75 ×14.5 0.138λ × 0.138λ	3.02-15.89	12.87	1.60	UWB
[36]	39 × 40 × 1.6 0.330λ × 0.339λ × 0.014λ	2.54 -12.08	9.54	2.14	UWB
proposed	20 × 20 × 1.6 0.187λ × 0.187λ × 0.016λ	2.80–11	7.6 GHz	4	UWB

5. Conclusion

The proposed twofold spoon-shaped UWB antenna is designed and developed with a compact dimension of 20 × 20 × 1.6 mm^3. The overall performance of the designed antenna and it is decided that this antenna is appropriate to use UWB applications. Moreover, this antenna is supported in the frequency domain and time domain with proper characterization. Several antenna parameters are optimized of the proposed antenna to improve the bandwidth, radiation pattern, gain. The proposed prototype reaches sufficient 121.67% fractional bandwidth on the ultra-wideband frequency range (2.80–11GHz) with a higher gain (5.80 dBi), a stable directional radiation pattern, and significant efficiency. Therefore, this article introduces a UWB antenna comprising a twofold spoon-shape radiating patch and inverted cone-shaped ground plane. The exploration of the simulation and measured results reveals that the proposed prototype is applicable for highly wideband applications.

Acknowledgement

This work is supported by the Universiti Kebangsaan Malaysia research grant GUP-2019-005.

References

[1] M. O'Halloran, D. Byrne, R. C. Conceição, E. Jones, M. Glavin, "Anatomy and Dielectric Properties of the Breast and Breast Cancer," in An Introduction to Microwave Imaging for Breast Cancer Detection: Springer, 2016, pp. 5-16.
[2] M. Aktar, M. M. Rana, M. S. Hossain, M. B. Hossain, Journal of Sensor Technology **9**(4), 91 (2019).
[3] Y.-S. Li, X.-D. Yang, Q. Yang, C.-Y. Liu, AEU-International Journal of Electronics and Communications **65**(11), 961 (2011).
[4] A. M. Abbosh, M. E. Bialkowski, IEEE Transactions on Antennas and Propagation **56**(1), 17 (2008).
[5] R. Sanyal, P. P. Sarkar, S. Sarkar, AEU-International Journal of Electronics and Communications **110**, 152833 (2019).
[6] A. A. H. Siddique, R. Azim, M. T. Islam, International Journal of Microwave and Wireless Technologies **11**(7), 711, (2019).
[7] M. Min, L. Guo, W. Che, W. Yang, "A Miniaturized Ultra-Wideband Dipole Antenna Utilizing A Concaved Arm," in 2019 IEEE MTT-S International Wireless Symposium (IWS), 2019: IEEE, pp. 1-3.
[8] K. Karthika, C. Kavitha, S. Yogahariharan, M. Shobikajanani, S. Harish, "Design of A Compact Staircase Shaped Ultra Wideband Antenna For Wireless Applications," in 2019 5th International Conference on Advanced Computing & Communication Systems (ICACCS), 2019: IEEE, pp. 468-471.
[9] R. Prasanna, N. M. Banu, Radioelectronics and Communications Systems **62**(4), 189 (2019).
[10] J. Meiguni, D. Pommerenke, IEEE Transactions on Antennas and Propagation **67**(10), 6371 (2019).
[11] S. Singh, V. Gupta, A. Kumar, Int. J. Eng. Res. Tech. **3**(5), 538 (2014).
[12] B. L. Shahu, S. Pal, N. Chattoraj, Frequenz **70**(3-4), 113 (2016).
[13] R. Azim, M. T. Islam, N. Misran, Applied Computational Electromagnetics Society Journal **26**(10), 856 (2011).
[14] M. Islam, M. Islam, M. Samsuzzaman, M. Faruque, N. Misran, Microwave and Optical Technology Letters **57**(11), 2580 (2015).
[15] D. Lee, W. Melek, G. Shaker, Microwave and Optical Technology Letters **61**(4), 1070 (2019).
[16] R. S. A. Anooz, African Journal of Engineering Research **7**(1), 10 (2019).
[17] M. Akbari, M. Koohestani, C. Ghobadi, J. Nourinia, International Journal of RF and Microwave Computer-Aided Engineering **21**(2), 216 (2011).
[18] A. Hachi, H. Lebbar, M. Himdi, D. Kurup, FE Journal of Electronics and Communications **21**(1-2), 53 (2019).
[19] M. Z. Mahmud, M. T. Islam, A. F. Almutairi, M. Samsuzzaman, U. Acharjee, M. T. Islam, Electronics **8**(4), 434 (2019).
[20] D. H. Werner, S. Ganguly, IEEE Antennas and Propagation Magazine **45**(1), 38 (2003).
[21] H. Nazli, E. Bicak, B. Turetken, M. Sezgin, IEEE Antennas and Wireless Propagation Letters **9**, 264 (2010).
[22] K.-H. Kim, S.-O. Park, IEEE Transactions on Antennas and Propagation **54**(6), 1688 (2006).
[23] J. Bai, S. Shi, D. W. Prather, IEEE Transactions on Microwave Theory and Techniques **59**(4), 1051 (2011).
[24] D. Schaubert, S. Kasturi, A. Boryssenko, W. Elsallal, "Vivaldi antenna arrays for wide bandwidth and electronic scanning," in The Second European Conference on Antennas and Propagation, EuCAP 2007, 2007: IET, pp. 1-6.
[25] T. Saktioto, M. Kurnia, R. Syahputra, M. Aziz, J. Ali, S. Punthawanunt, P. Yupapin, International Journal of Pure and Applied Mathematics **119**(15), 2477 (2018).
[26] B. Sahu, S. Singh, M. K. Meshram, S. Singh, Journal of Electromagnetic Waves and Applications **33**(1), 107 (2019).
[27] R. Mondal, P. S. Reddy, D. C. Sarkar, P. P. Sarkar, IET Microwaves, Antennas & Propagation **14**(1), 66 (2020).
[28] C. A. Balanis, E. Holzman, "Circular waveguides," Encyclopedia of RF and Microwave Engineering, 2005.
[29] K. U. Sam, P. Abdulla, Progress in Electromagnetics Research C **99**, 111 (2020).
[30] J. Tao, Q. Y. Feng, Journal of Electromagnetic Waves and Applications **30**(16), 2206 (2016).

[31] S. Kundu, S. K. Jana, Microwave and Optical Technology Letters **60**(4), 930 (2018).
[32] R. Azim, M. T. Islam, N. Misran, Arabian Journal for Science and Engineering **38**(9), 2415 (2013).
[33] R. Azim, A. Mobashsher, M. T. Islam, Electronics Letters **49**(15), 922 (2013).
[34] R. Azim, M. T. Islam, N. Misran, Telecommunication Systems **52**(2), 1171 (2013).
[35] R. Azim, M. T. Islam, N. Misran, A. T. Mobashsher, Informacije MIDEM **41**(1), 37 (2011).
[36] R. Azim, M. T. Islam, N. Misran, "Printed circular ring antenna for UWB application," in International Conference on Electrical & Computer Engineering (ICECE 2010), 2010: IEEE, pp. 361-363.

*Corresponding author: ismailiiuc555@gmail.com,
sobuz@pstu.ac.bd,
tariqul@ukm.edu.my